AFRL-RV-PS-
TR-2017-0005

CHARACTERIZATION OF RAIN ATTENUATION AND DEPOLARIZATION AT W/V BANDS

Christos Christodoulou

University of New Mexico
1 University of New Mexico
Albuquerque, NM 87131

22 Mar 2017

Final Report

AIR FORCE RESEARCH LABORATORY
Space Vehicles Directorate
3550 Aberdeen Ave SE
AIR FORCE MATERIEL COMMAND
KIRTLAND AIR FORCE BASE, NM 87117-5776

DTIC COPY

NOTICE AND SIGNATURE PAGE

Using Government drawings, specifications, or other data included in this document for any purpose other than Government procurement does not in any way obligate the U.S. Government. The fact that the Government formulated or supplied the drawings, specifications, or other data does not license the holder or any other person or corporation; or convey any rights or permission to manufacture, use, or sell any patented invention that may relate to them.

This report is the result of contracted fundamental research deemed exempt from public affairs security and policy review in accordance with SAF/AQR memorandum dated 10 Dec 08 and AFRL/CA policy clarification memorandum dated 16 Jan 09. This report is available to the general public, including foreign nationals. Copies may be obtained from the Defense Technical Information Center (DTIC) (http://www.dtic.mil).

AFRL-RV-PS-TR-2017-0005 HAS BEEN REVIEWED AND IS APPROVED FOR PUBLICATION IN ACCORDANCE WITH ASSIGNED DISTRIBUTION STATEMENT.

//SIGNED//
DAVID MURRELL
Program Manager

//SIGNED//
DAVID CARDIMONA
Technical Advisor, Space Based Advanced Sensing and Protection

//SIGNED//
JOHN BEAUCHEMIN
Chief Engineer, Spacecraft Technology Division
Space Vehicles Directorate

This report is published in the interest of scientific and technical information exchange, and its publication does not constitute the Government's approval or disapproval of its ideas or findings.

REPORT DOCUMENTATION PAGE

Form Approved
OMB No. 0704-0188

1. REPORT DATE *(DD-MM-YYYY)*	**2. REPORT TYPE**	**3. DATES COVERED** *(From - To)*
22-03-2017	Final Report	12 Aug 2015 to 9 Feb 2017

4. TITLE AND SUBTITLE
Characterization of Rain Attenuation and Depolarization at W/V Bands

5a. CONTRACT NUMBER
FA9453-15-1-0319

5b. GRANT NUMBER

5c. PROGRAM ELEMENT NUMBER
63401F

6. AUTHOR(S)
Christos Christodoulou

5d. PROJECT NUMBER
682J

5e. TASK NUMBER
PPM00015184

5f. WORK UNIT NUMBER
EF126322

7. PERFORMING ORGANIZATION NAME(S) AND ADDRESS(ES)
University of New Mexico
1 University of New Mexico
Albuquerque, NM 87131

8. PERFORMING ORGANIZATION REPORT NUMBER

9. SPONSORING / MONITORING AGENCY NAME(S) AND ADDRESS(ES)
Air Force Research Laboratory
Space Vehicles Directorate
3550 Aberdeen Ave SE
Kirtland AFB, NM 87117-5776

10. SPONSOR/MONITOR'S ACRONYM(S)
AFRL/RVSW

11. SPONSOR/MONITOR'S REPORT NUMBER(S)
AFRL-RV-PS-TR-2017-0005

12. DISTRIBUTION / AVAILABILITY STATEMENT
Approved for public release; distribution is unlimited.

13. SUPPLEMENTARY NOTES

14. ABSTRACT
The use of W/V band for applications in mobile communications as well as high bandwidth satellite links continues to build across industry and governments. However, developments in modeling of atmospheric attenuation and research into antennas that operate at these frequencies are in relative infancy compared to the more commonly used bands. This effort investigates both the validity of current attenuation models for W/V band as well as investigating a novel slot antenna design. The published W/V band attenuation model by the International Telecommunications union (ITU) was found to be lacking based on experimental validation. Furthermore, the W/V band slot antenna design and subsequent arrays in this work were simulated and show promise as a useful radiator.

15. SUBJECT TERMS
W/V band; Attenuation Research; Slot Antenna; Array Development

16. SECURITY CLASSIFICATION OF:			**17. LIMITATION OF ABSTRACT**	**18. NUMBER OF PAGES**	**19a. NAME OF RESPONSIBLE PERSON**
a. REPORT	**b. ABSTRACT**	**c. THIS PAGE**			David A. Murrell
Unclassified	Unclassified	Unclassified	Unlimited	32	**19b. TELEPHONE NUMBER** *(include area code)*

(This page intentionally left blank)

TABLE OF CONTENTS

LIST OF FIGURES

LIST OF TABLES

ACKNOWLEDGMENTS

This material is based on research sponsored by Air Force Research Laboratory under agreement number FA9453-15-1-0319. The U.S. Government is authorized to reproduce and distribute reprints for Governmental purposes notwithstanding any copyright notation thereon.

DISCLAIMER

The views and conclusions contained herein are those of the authors and should not be interpreted as necessarily representing the official policies or endorsements, either expressed or implied, of Air Force Research Laboratory or the U.S. Government.

(This page intentionally left blank)

1.0 SUMMARY

The use of W/V band for applications in mobile communications as well as high bandwidth satellite links continues to build across industry and governments. However, developments in modeling of atmospheric attenuation and research into antennas that operate at these frequencies are in relative infancy compared to the more commonly used bands. This effort investigates both the validity of current attenuation models for W/V band as well as investigating a novel slot antenna design. The published W/V band attenuation model by the International Telecommunications Union (ITU) was found to be lacking based on experimental validation. Furthermore, the W/V band slot antenna design and subsequent arrays in this work were simulated and show promise as a useful radiator.

2.0 INTRODUCTION

The most critical problem in the W/V band type of communication link is the uncertainty of signal attenuation, depolarization, and phase distortion that results from atmospheric absorption, scintillation, and meteorological effects (e.g., rain fade, atmospheric and molecular absorption, etc.) [1-6]. Rain parameters such as drop size, drop shape and canting affect the propagation of waves at such extremely-high frequencies. Rain is the most dominant attenuation cause and scattering in the atmosphere at W/V band. At these frequencies, the wavelength is comparable to the size of raindrops. As rainfall affects the propagation of the wave, rainfall itself is also affected by several other factors, such as wind velocity and temperature.

Some of our previously reported work focused on validating the Mie theory for rain attenuation at 72 and 84 GHz. We compared model predictions under various parameters such as complex index of refraction models and raindrop size distribution models to experimental data. The data was collected from the W/V band Terrestrial Link Experiment (WTLE) that has been in operation between the Sandia Crest and the University of New Mexico since the summer of 2015. The distance between the transmitter and the receiver is approximately 22.5 km with an elevation angle of 4.16 degrees. Two different models, the International Telecommunication Union Radio communication Sector ITU-R [1] and the Siva-Mello [4] models, were used to predict attenuation. Some of the results were reported last year. This year a shorter distance prototype of the WTLE experiment was established, spanning the distance of only 0.56 km and operating at 84 GHz. In this experiment the weather factors affecting any signal attenuation are better known than the

longer version of the WTLE experiment.

This report is divided into three parts. The first part covers the results from the data analyzed from the short link to examine the validity and the accuracy of the ITU-R and Silva models for rain attenuation for the Albuquerque, New Mexico region. The second part covers a preliminary antenna array design that is being developed at the W/V band that can be used in future communication links. The third part includes the study of a circular horn antenna design for high gain performance at W/V band frequencies.

The report ends with a conclusion stating the nature of this on-going work and the future research to be completed.

3.0 METHODS, ASSUMPTIONS AND PROCEDURES

3.1 W/V Band Attenuation Modeling

To overcome the ambiguity caused by the missing weather data over the 22.5 km link, and to have better control over the experiment, a short link of 0.56 km operating at 84 GHz was built. The 84 GHz receiver located at the top of the Space Electronics Center at the University of New Mexico (COSMIAC) building that is used for the WTLE experiment was redirected to serve as the receiver for the short link experiment. An 84 GHz transmitter was placed on top of the Schafer Corporation building. The equipment locations are shown in Figure 1 Rain rate and received power are still recorded at the receiver site. In this case, the rain rate seen at the receiver can be assumed to be uniform for the overall link because the communication path is short. The data used for the short link analysis spans roughly from August 3, 2016 till September 30, 2016. The same ITU-R model [5-9] used in the Long link analysis is tested in this short link experiment. Even though the sample size is small, it is sufficient in order to perform a preliminary test to check whether the ITU-R model is accurate for the region of Albuquerque or not. In this report we show:

1) A comparison of the measured rain attenuation relative to clear air and the calculated rain attenuation based on the ITU-R model [5-9] exceeded for 0.01% of the time and 0.1% of the time at 84 GHz.

2) A comparison of the measured rain attenuation relative to clear air and the calculated rain attenuation based on the ITU-R model as a function of the rain rate, and finding new k and α coefficients for the ITU-R model to fit it to the experimental results.

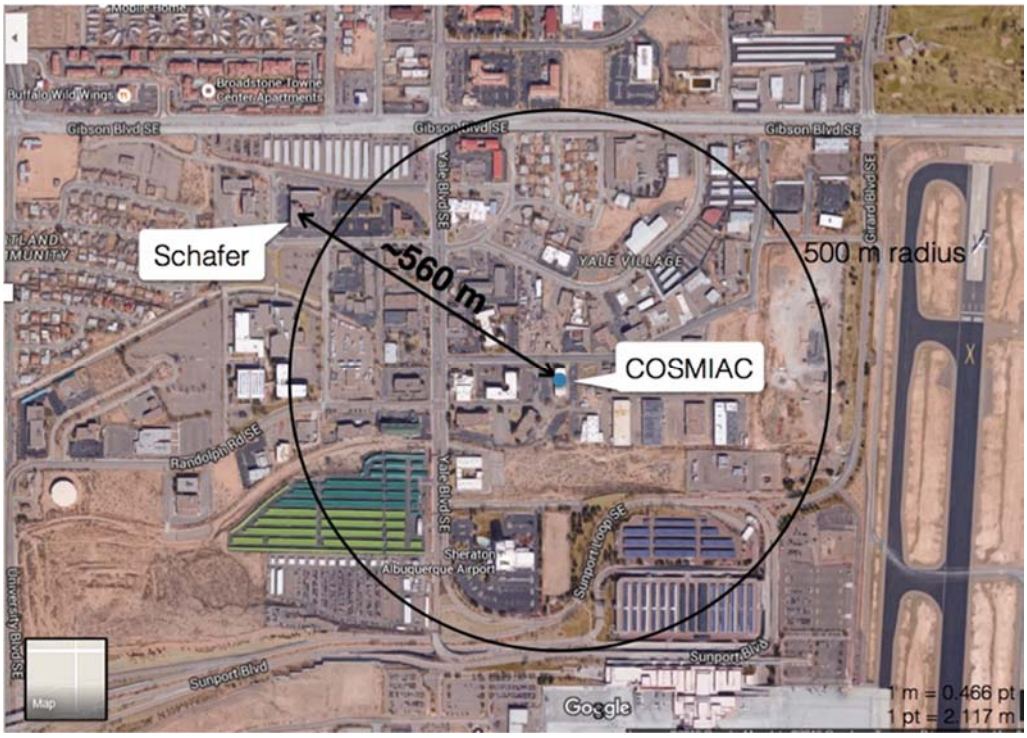

Figure 1. Short Link Experiment Location

3.2 Cross Slotted Waveguide

The idea of the cross slotted waveguide was introduced by A.J. Simmons [10]. The position of the slot on the broad-wall creates the circular polarization. At this position, the $\vec{H}$ field has two components that are orthogonal, with equal magnitudes and 90° out of phase:

$$H_x = \frac{j\beta m\pi}{k_c^2 a} A_{mn} \sin\left(\frac{m\pi x}{a}\right) \cos\left(\frac{n\pi y}{b}\right) e^{-j\beta z} \quad (1)$$

$$H_y = \frac{j\beta n\pi}{k_c^2 b} A_{mn} \cos\left(\frac{m\pi x}{a}\right) \sin\left(\frac{n\pi y}{b}\right) e^{-j\beta z}$$

$$H_z = A_{mn} \cos\left(\frac{m\pi x}{a}\right) \cos\left(\frac{n\pi y}{b}\right) e^{-j\beta z}$$

Since the slot is at the broad-wall, and disregarding the phase component, the field's values are:

$$H_x = \pm \frac{j\beta m\pi}{k_c^2 a} A_{mn} \sin(\frac{m\pi x}{a})$$

$$H_x = 0 \tag{2}$$

$$H_z = \pm A_{mn} \cos(\frac{m\pi x}{a})$$

The two components of the magnetic field on the broad-wall are 90° out of phase for all values of x.

For a TE_{10} mode, $k_c = \frac{m\pi}{a}$ and $\beta = \sqrt{k^2 - k_c^2} = \sqrt{\omega^2 \mu\varepsilon - (\frac{m\pi}{a})^2}$

In order to find the values of x for which the circular polarization can be achieved, the following equation should be solved:

$$|H_x| = |H_z|$$

$$\frac{\beta\pi}{k_c^2 a} A_{10} \sin\left(\frac{\pi x}{a}\right) = A_{10} \cos(\frac{\pi x}{a}) \tag{3}$$

$$\tan\left(\frac{\pi x}{a}\right) = \frac{k_c^2 a}{\beta\pi} \quad with\ x \neq a/2.$$

The value of x where circular polarization at a certain frequency f can be achieved can be found using the following equation:

$$x = \pm \frac{a}{\pi} \times tan^{-1}\left(\frac{1}{\sqrt{\left(\frac{2fa}{c}\right)^2 - 1}}\right) + na\ where\ n = 0\ or\ 1 \tag{4}$$

This equation shows that there are two values for x, on the broad-wall, where circular polarization can be achieved. The two positions are symmetrical with respect to the center line of the broad-wall. At these positions, the H_x component is either leading or lagging by 90°. This property of the cross slotted waveguide antenna allows for Left Hand Circular Polarization (LHCP) or Right Hand Circular Polarization (RHCP) wave to be radiated. Dual polarization can be achieved by switching the feed from one end of the waveguide to the other end. In Figure 2, the positions where the circular polarization can be achieved at their corresponding frequencies for a WR10 rectangular waveguide are shown. In order to radiate power out of the waveguide, cross slots on the broad-wall can be placed, with their centers positioned at the positions x. The cross slot arms should be perpendicular to each other, forming an angle of 45° with the broad-wall edges. The length of each arm should be $L_a \approx \lambda/2$.

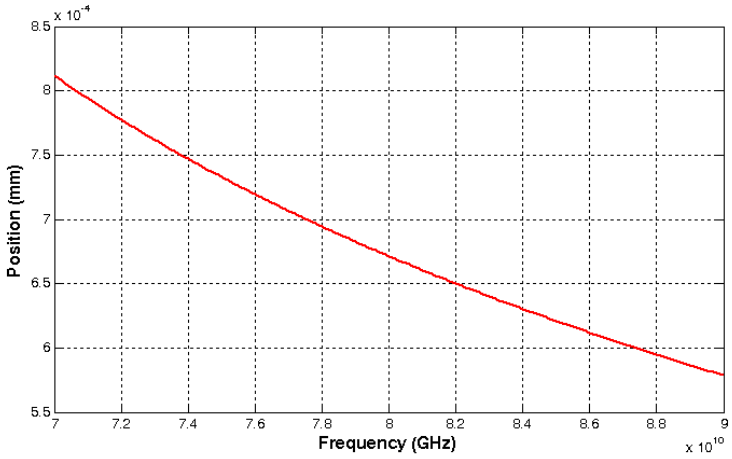

Figure 2: The computed x positions for a WR10 rectangular waveguide.

Waveguide with One Slot.

The same design suggested by Simmons was done at W/V band frequencies. A WR10 rectangular waveguide is used. The waveguide dimensions are a = 2.54 mm and b = 1.27 mm. The cross slot is located in the broad-wall at a position of x = 0.715 mm from the narrow wall. The waveguide is fed by 2 ports from each side for different circular polarizations. The slot arm has L_a = 2.05mm corresponding to a resonant frequency of 84 GHz and a slot width of W_a = 0.127 mm. The arms are perpendicular to each other and form an angle $\alpha = 45^o$ with the wall of the waveguide as shown in Figure 3a. The one slot produces a gain of 3.4 dB at 85.5 GHz, with a left hand to right hand circular polarization ratio of 20 dB at the direction of maximum gain.

It was noticed that the design of such an antenna has limitations in terms of the frequencies where circular polarization can be achieved. These limitations are caused by the length of the slot arm and the position of the center of the slot. In certain cases, the arm length doesn't fit inside the waveguide walls especially at lower frequencies where the lengths are higher. In order to solve this problem, the slot shown in Figure 3b is proposed. The arms have a Z shape, where the curved sections are small enough to create the same resonance length, and also keep the circular polarization property of the antenna.

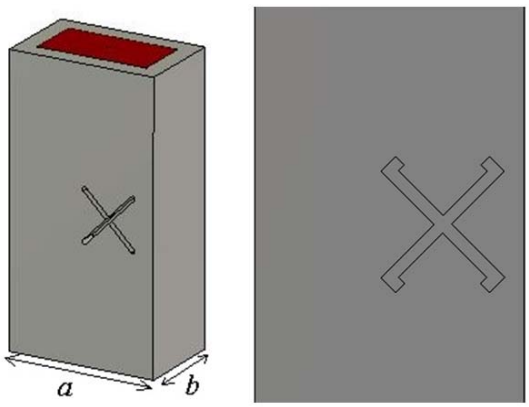

Figure 3. a) Straight arm slot, b) Z arm slot.

4.0 RESULTS AND DISCUSSION

4.1 W/V Band Modeling

First, the rain attenuation according to the ITU-R model was calculated. The cumulative distribution function cumulative distribution function (CDF) for the rain rate is shown in Figure 4. The rain rate exceeded for 0.1% of the time is 13.715 mm/hr and the rain rate exceeded for 0.01% of the time is 129.29 mm/hr.

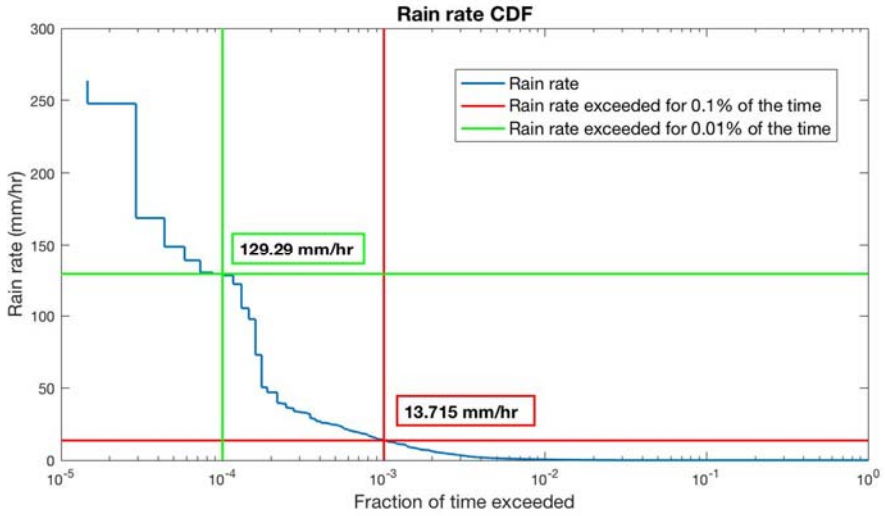

Figure 4. Short Link Rain Rate Cumulative Distribution Function

The calculated rain attenuation exceeded for 0.1% of the time at 84 GHz is 8.344 dB and the calculated rain attenuation exceeded for 0.01% of the time at 84 GHz is 34.734 dB according to the ITU-R model.

4.1.1 Measured Attenuation

Second, the attenuation according to the received experimental power was calculated. The noise floor level for this link, at 84 GHz, is -80 dBm. The same procedure as the one considered for the long link was followed to assess which data are useful to keep for the experiment and which data should be deleted due to any failures in the equipment or any improbable events in the experiment.

The CDF for the total measured attenuation is shown in Figure 5. The clear air attenuation seen for 90% of the time is 20.202 dBm. The total attenuation exceeded for 0.1% of the time is 43.192 dBm and the total attenuation exceeded for 0.01% of the time is 58.857

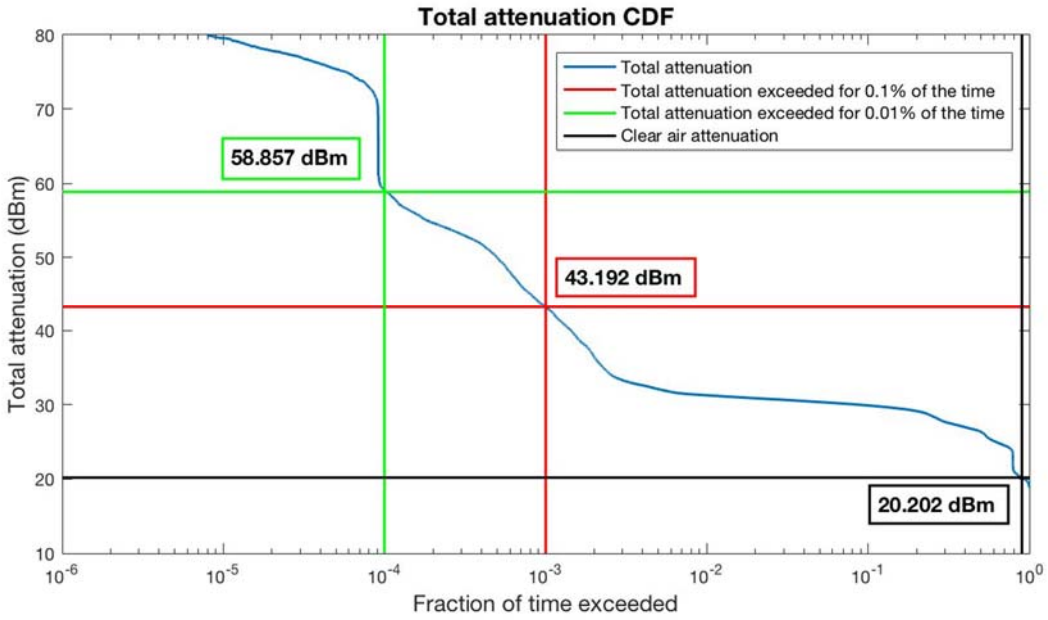

Figure 5. Short Link Total Measured Attenuation Cumulative Distribution Function at 84 GHz

The rain attenuation relative to clear air is calculated using equation 2.1.

$$rain\ attenuation\ relative\ to\ clear\ air = total\ attenuation\ -\ clear\ air\ attenuation \quad (5)$$

Therefore, the rain attenuation relative to clear air exceeded for 0.1% of the time is 22.99 dB and the rain attenuation relative to clear air exceeded for 0.01% of the time is 38.655 dB.

Next, the dynamic range is calculated using equation 2.2.

$$dynamic\ range = clear\ air\ attenuation - noise\ floor$$

$$dynamic\ range = \ 20.202 \ - \ (-80) \tag{6}$$

$$dynamic\ range = \ \ 100.202\ dB$$

4.1.2 Results Analysis

Once again, the values resulting from the ITU-R model calculations and the experimental results are compared. The difference is calculated according to equation 2.3. The results are summarized in Table 1.

$$\%\ difference = \frac{Experimental\ rain\ attenuation - ITUR\ rain\ attenuation}{ITUR\ rain\ attenuation} \times 100 \tag{7}$$

Table 1. Short Link Comparison of ITU-R and Experimental Results

Fraction of time exceeded	Rain rate (mm/hr)	ITU-R rain attenuation (dB)	Experimental rain attenuation (dB)	Percentage difference
0.1%	13.715	8.344	22.99	175.53%
0.01%	129.29	34.734	38.655	11.29%

The ITU-R model seems to underestimate the rain attenuation compared to the real values. The difference between the ITU-R model results and the experimental results is more severe at low rain rate than at higher rain rates. Thus, it is obvious that the ITU-R model is not accurate for the WTLE experiment conducted in Albuquerque, New Mexico.

4.2 Fitting of ITU-R Model

The k and α coefficients used in the analysis so far are given by the ITU-R model. However, these coefficients are highly dependent on climate conditions and cannot be assigned one single value to cover any experiment, independently of the region where the experiment is conducted. Conversely, the climate regime of the region under consideration should be taken into account to find the appropriate values of the k and α coefficients to check if the ITU-R model can correctly

estimate the experimental signal attenuation. Therefore, in the following section, the least square error fitting method was used to fit the ITU-R model to the experimental results. Originally, the k and α coefficients given by the ITU-R at 84 GHz are the following:

$k = 1.2164$

$\alpha = 0.6999$

After fitting the experimental values, it turns out that the corrected k and α coefficients, with a 95% confidence bounds, that should be used with the ITU-R model to calculate the attenuation for the WTLE link are the following:

$k = 17.5 \quad (17.18,\ 17.82)$

$\alpha = 0.06003 \ (0.05796,\ 0.0621)$

Figure 6 shows the measured attenuation as a function of rain rate, the original calculated attenuation using the k and α coefficients suggested by the ITU-R model, and the fitted attenuation corresponding specifically to the short link experiment. A Korean group tested the ITU-R model for rain attenuation at 73 GHz and 83 GHz over a short 0.5 km terrestrial link. They proved that the ITU-R model showed a good estimate for the rain rates below 100 mm/hr, but it was inconsistent for the rain rates above 100 mm/hr.

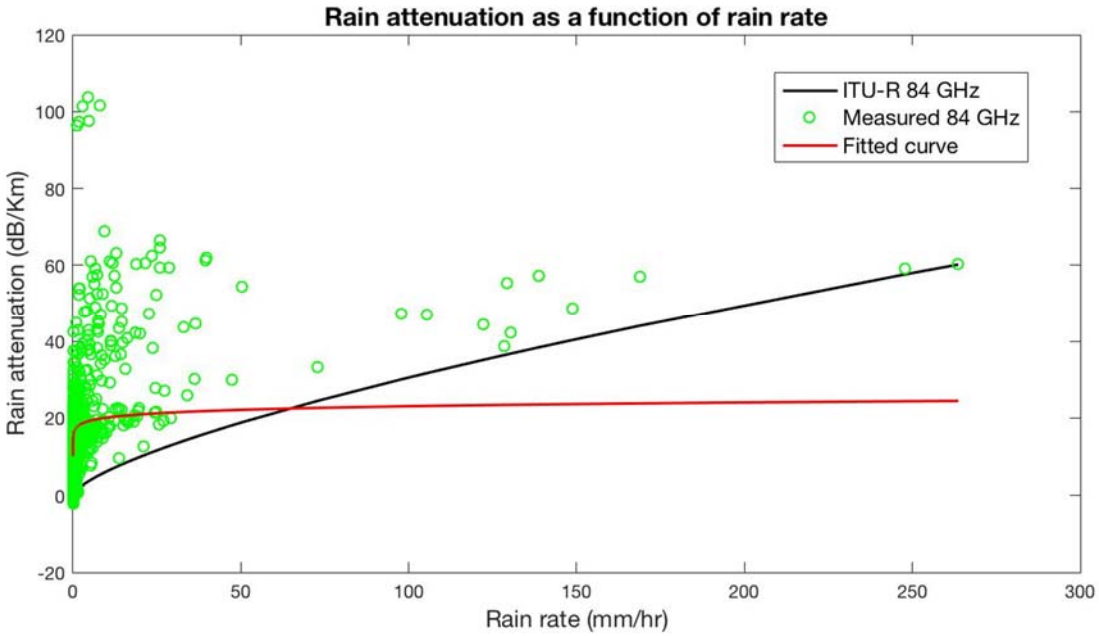

Figure 6. Rain Attenuation as a Function of Rain Rate

The attenuation according to the ITU-R model was calculated again using the k and α coefficients found from the curve fitting procedure. The new calculations show that the calculated rain attenuation exceeded for 0.1% of the time is 26.342 dB and the attenuation exceeded for 0.01% of the time is 29.751 dB. To check if these new coefficients showed some improvement to the ITU-R model, the results are summarized in Table 2.

Table 2. Comparison of ITU-R Model before fitting and after fitting

Fraction of time exceeded	Rain rate (mm/hr)	Percentage difference with old k and α	Percentage difference with new k and α
0.1%	13.715	175.53%	-12.72%
0.01%	129.29	11.29%	29.93%

When the rain rate is 13.715 mm/hr, at the lower limit of the heavy rain rate category according to Table 3 the fitted curve showed significant improvement in matching the ITU-R model to the experiment compared to the results noted previously when using the original k and α coefficients values. However, when the rain rate is 129.29 mm/hr, which is categorized as violent rain rate according to Table 3, the fitted curve coefficients resulted in a worse matching than the one gotten when using the original k and α coefficients with the ITU-R model.

Table 3. Rain Rates Categories

Description	Rain rate (mm/hr)
Light Rain	0 – 2
Moderate Rain	2 – 10
Heavy Rain	10 – 50
Violent Rain	> 50

Albuquerque is in the lower half of the heavy rain rate category. It is clearly noticeable from Figure 6 that the majority of the rain events occur between 0 and 25 mm/hr. A larger set of data is needed to validate any theory, however as a preliminary finding, the power law, $\gamma_R = k\, R^{\alpha}$ given by the ITU-R to calculate the rain attenuation, cannot be fitted to the real data for the Albuquerque region. A different equation having a steeper slope for low rain rates and a slope converging to saturation at high rain rates must be generated.

In general, the ITU-R model for rain attenuation proved to be invalid for the WTLE experiment. This model depends highly on the k and α coefficients that in turn depend on the

frequency of operation and on the rain regime of the region of interest. Even when trying to fit these coefficients to the experiment using the least square error, a general result satisfying low rain rates and high rain rates could not be found. A new form of the equation might be needed to account for the special climate conditions in Albuquerque, New Mexico.

The WTLE experiment is an ongoing project, more resources will be added continuously to help improve the accuracy of the experiment and the effects of the weather conditions on the propagating signal in more depth. Some of the expected improvements in the future are, adding disdrometers and weather stations at different locations along the path to have a better understanding of the climate conditions all over the path, and adding a fog sensor at the transmitter site on top of the Sandia Peak to be able to monitor the clouds effect on the signal.

4.3 Slot Waveguide Array

A single slot waveguide like the one shown in Figure 3. doesn't radiate enough power so an array was designed. The array has 8 slots. The higher number of slots produces higher gain and enables the antenna to radiate more power. The slot total length was L = 1.85 mm with the small section's length L_s = 0.15 mm. The separation between the slots was S = λ/2. The array is shown in Figure 7a.

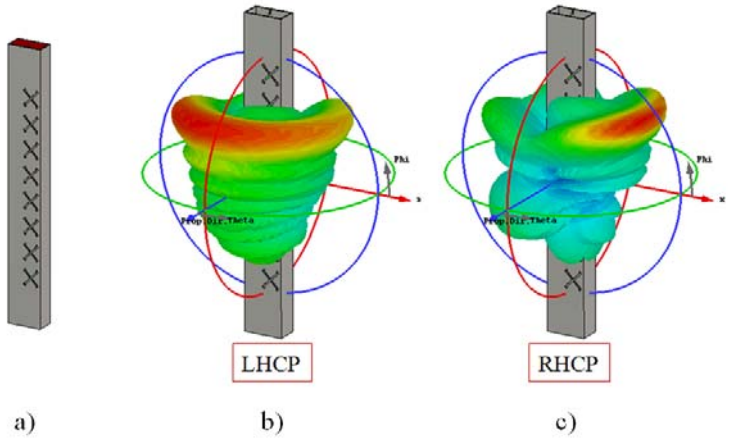

Figure 7a) The Z arm slot array antenna, b) the Left Hand Circularly Polarized (LHCP) 3D radiation Pattern at 84.75 GHz and c) the Right Hand Circularly Polarized (RHCP) 3D radiation Pattern at 84.75 GHz

The simulation of the array was done using CST Microwave Studio. The array was fed by 2-ports separately. Each port produces a different circular polarization. The simulation showed good antenna operability at 85.5 GHz. The antenna S-parameters showed that the antenna is well matched between 75-90 GHz. At 85.5 GHz more than 90% of the power is radiated and the antenna is well matched at the input as shown in Figure 8. The radiation pattern of this antenna at 85.5 GHz

showed a gain of 11.6 dB for LHCP and the isolation between left handed LH and right handed RH circular polarization was -18.5 dB in the direction of maximum gain. The side lobe level at this frequency is -12 dB as shown in Figure 9. The main beam is in the direction of $\theta = 39^{o}$. The gain at the main beam varies between 10-12 dB as shown in Figure 10.

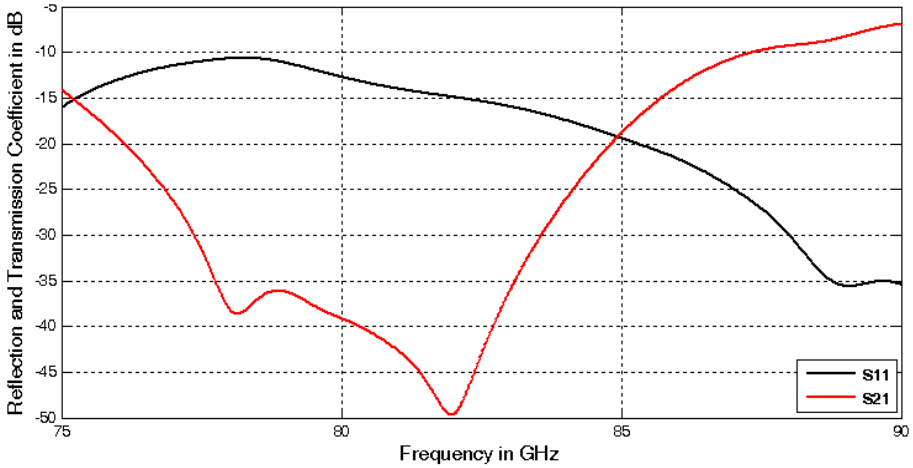

Figure 8. The reflection coefficient and the transmission from port 1 to port 2 of the array.

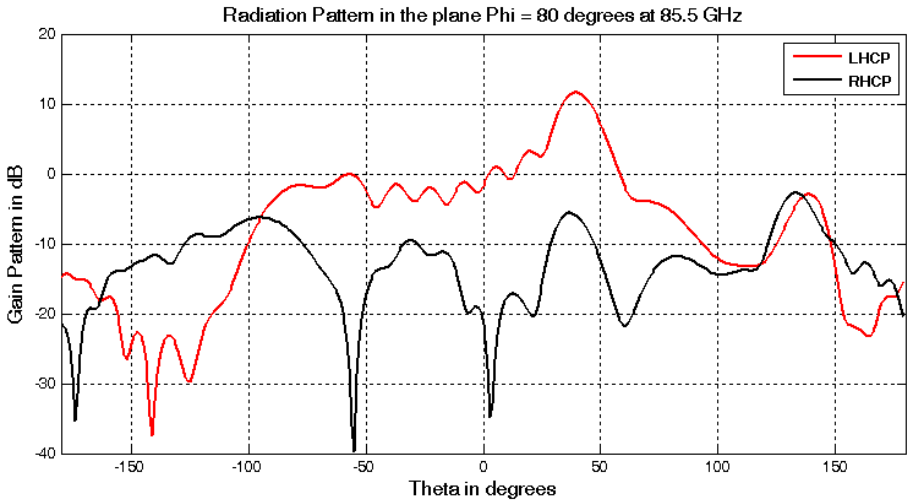

Figure 9. The radiation pattern of the antenna in the plane Phi =80 degrees.

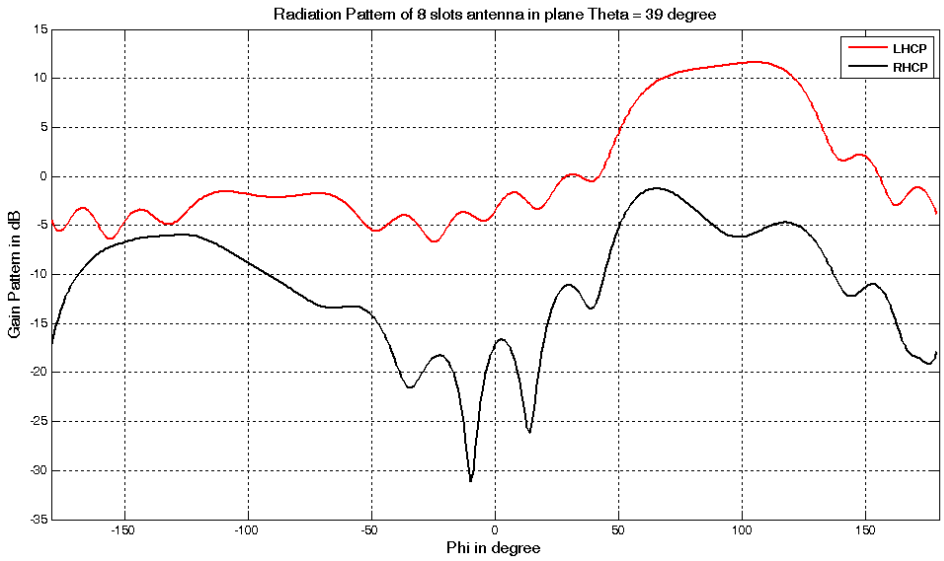

Figure 10. The radiation pattern of the antenna in the plane Theta = 39 degrees.

The problem with the single waveguide cross slot array was that the maximum radiation direction was not the same as the direction of the null on the main beam for the opposite circular polarization. In order to fix this problem, small horn cavities, or circular waveguide sections could be added around each slot.

4.3.1 2-D Array.

Expanding this array into 2 dimensions increases the gain by concentrating the radiation in one direction [11-13]. It also makes the entire half power beam-width circularly polarized. The problem with the 2-D array is the feeding and the phase between the waveguide elements. The study of the radiation pattern of the 2-D array using the array factor, showed that:

- The center waveguides should be fed in phase if the number of waveguides is even.
- The phase difference with the next in line waveguide (on both sides) should be low.
- The waveguides on either side of the center, should have the same phase.

An array of 3x16 was designed. The expected gain was 20 dB at 84 GHz. For the feeding network, a waveguide with 3 slots on the narrow wall was used as shown in Figure 11a and b. The slots have 360^{o} phase difference center to center. The first and third slot widths are 0.43 mm, and the middle slot has a width of 0.44 mm. The slot lengths are 1.88 mm. The slots radiate into 3 different waveguides. The center waveguide is a straight section waveguide. The other waveguides

are curved waveguides. The curvature of the waveguides was chosen in a way to minimize reflections. The third waveguide is a mirror about the center of the first waveguide. That secures the same phase difference that is added at the output of both waveguides. The feeding network largest length is 37.4 mm.

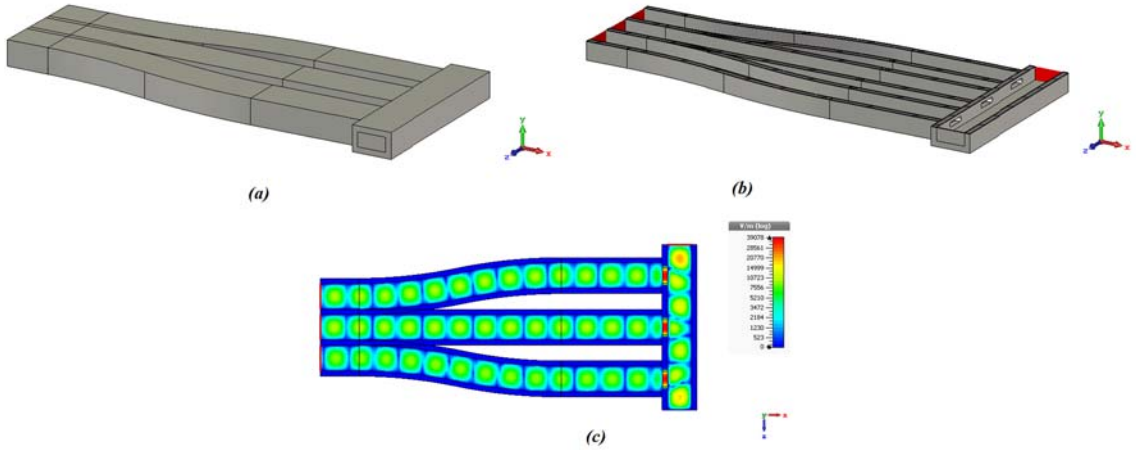

Figure 11. a) Feed Network Design, b) Interior Design of the Feed, and c) The E field inside the feed.

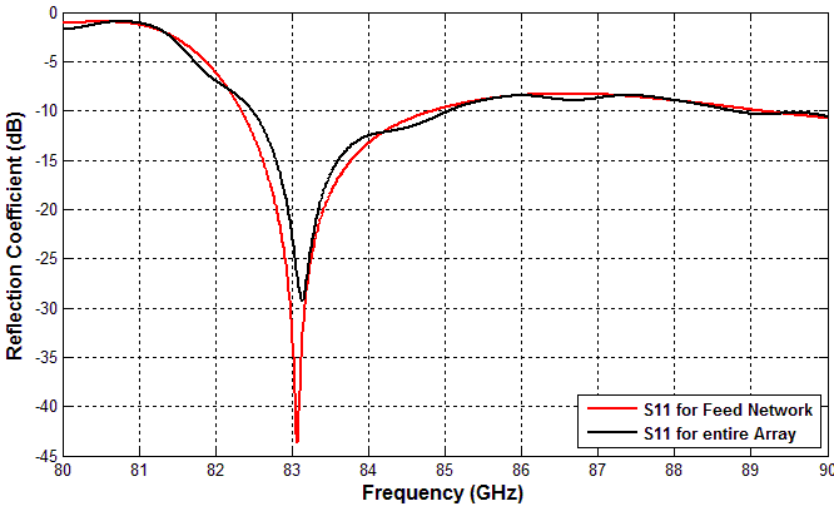

Figure 12. The reflection coefficient of the feed network, and the feed network with the array.

By examining the scattering parameters of the feed network, it was noticed that it is matched between 82.5 - 85 GHz as seen in Figure 12. The S_{21}, S_{31} and S_{41} have almost the same magnitude and phase between 82.5 - 85 GHz. This property secures a feeding in phase and with equal magnitudes (-5 dB) to all the waveguides of the array as seen in Figure 13 and 14.

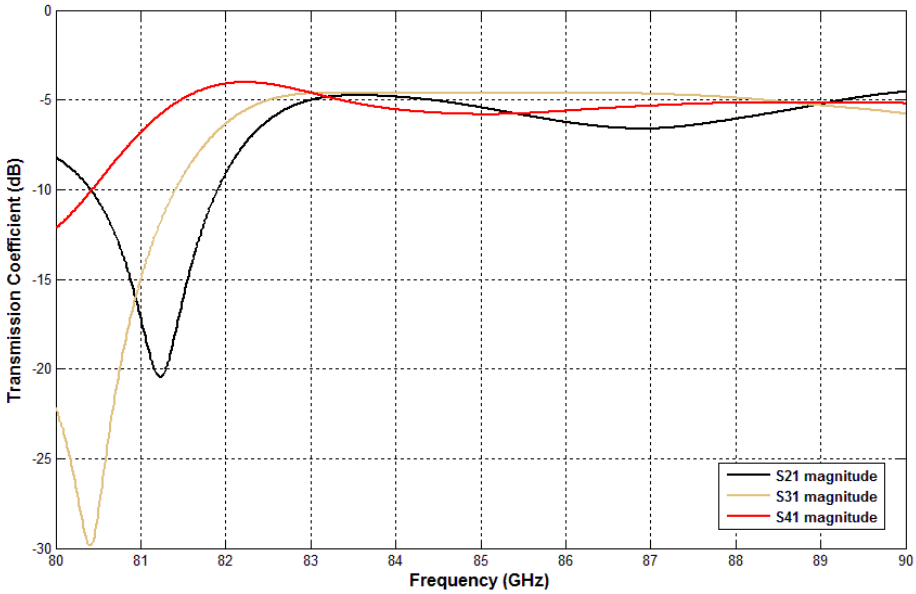

Figure 13. Transmission coefficient magnitudes.

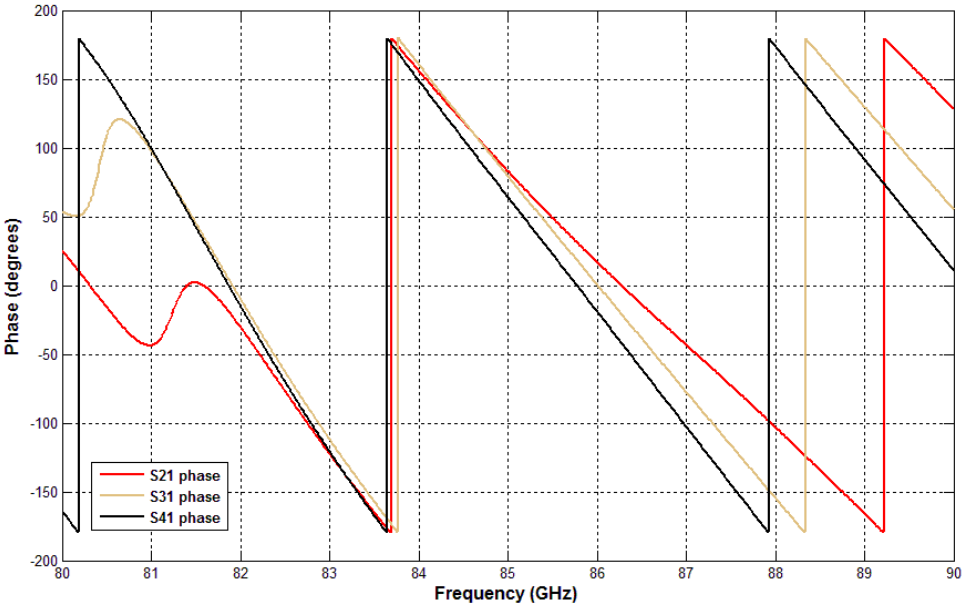

Figure 14. The phase plot of the transmission coefficients.

The feed network was then connected to the 3x16 slot array and the simulation of the entire design was done. A gain of 20.5 dB was achieved at 84 GHz. The individual waveguides were replicas of the design of the single waveguide presented in the previous section. The maximum gain is in the plane $\Phi = 90^{o}$ and at a direction $\theta = 40^{o}$ as shown in Figure 15. The radiation patterns' main lobe was almost in the same direction for frequencies between 82.5 - 85 GHz, which are the frequencies of operation of the design as seen in Figure 12.

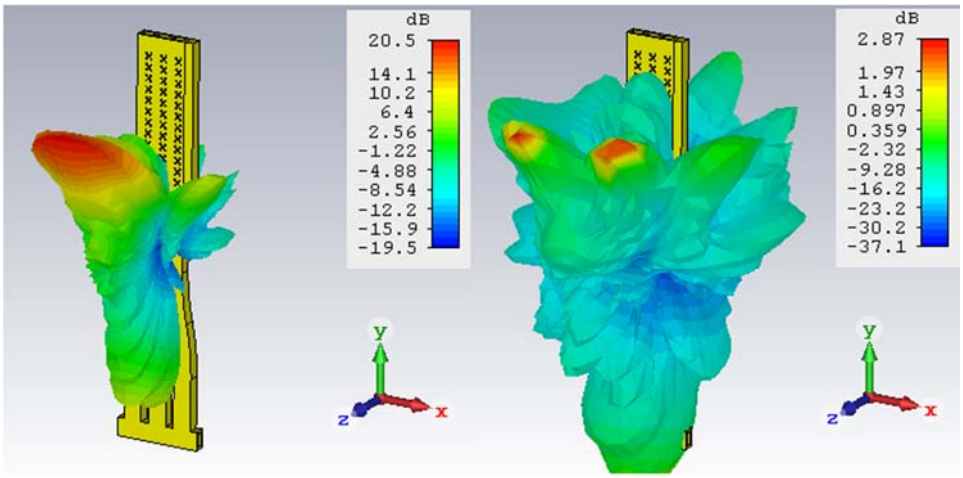

Figure 15. a) Left hand circularly polarized radiation pattern, b) right hand circularly polarized radiation pattern at 84 GHz.

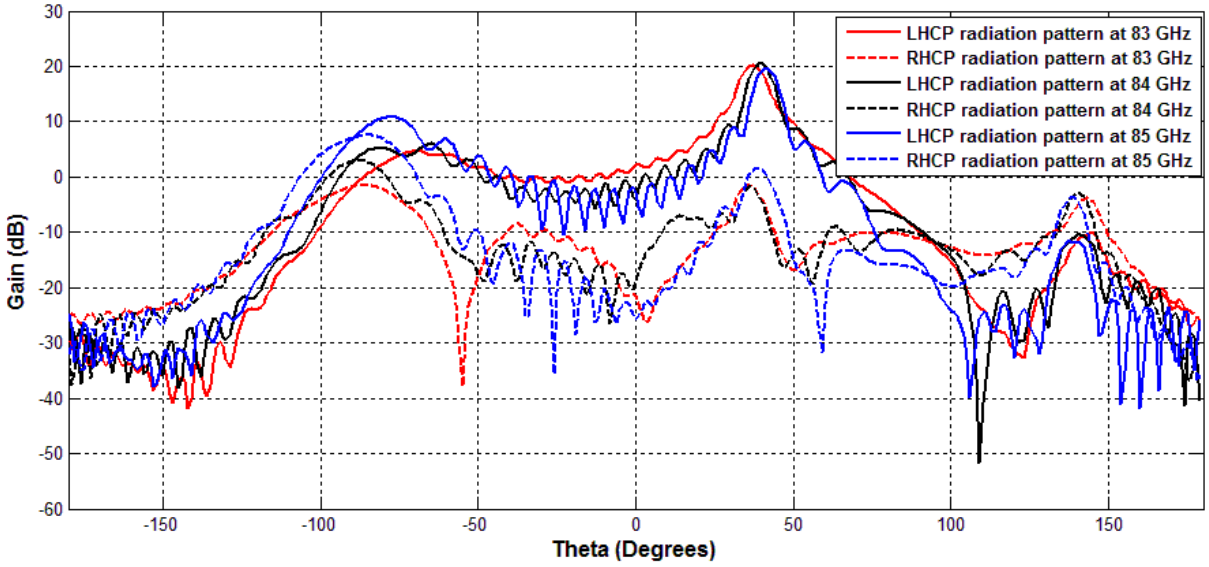

Figure 16. RHCP and LHCP radiation patterns at different frequencies.

As shown in Figure 16 the array has a gain of 20 dB between 83-85 GHz. The isolation between LH and RH circular polarizations at the maximum gain was more than 20 dB over the entire range of frequencies of operation. The side lobe level was less than 14 dB and the half power beam width is 8.4^o in the $\Phi = 90^o$ plane.

The problem with the design of waveguide slotted arrays is that, when the feeding port is switched in order to change the polarization, the beam direction also switches and hence if the target of communication is still at the same direction, the entire antenna direction should be

switched. In order to solve this problem, a horn antenna fed by one of the cross slots was designed next.

4.3.2 Circular Feed Extension.

The design of the array showed that the main beams of the different polarization senses are directed in different directions. This is caused by the phase difference at each slot. By switching the feeding port, the beam also switches. In order to solve this problem, the radiation generated by one slot can be extracted into either a square waveguide or a circular waveguide. These two types of waveguides were chosen because their fundamental modes, TE_{10} and TE_{01} in the case of the first and TE_{11} in the case of the second, can be excited in orthogonal directions with a 90^o phase difference. At the position of the cross slot, the $\vec{H}$ field has two components, H_x and H_z that are orthogonal and 90^o out of phase. These two components have their magnitudes almost equal for a large band of frequencies. This magnetic field is coupled through the cross slot into the extraction waveguide where the fundamental modes should be excited.

Here, a circular waveguide, with a TE_{11} mode operating was used for power extraction. Since the coupled field has two components H_x and H_z that are 90^o out of phase, two degenerate TE_{11} modes, that are orthogonal to each other and in quadrature phase difference, are excited. This wave, if radiated through a horn antenna, can create a circularly polarized radiation that points in the same direction for both polarization senses.

This same concept applies to a square waveguide that operates in its fundamental modes. The TE_{10} and TE_{01} modes are excited with a 90^o phase difference between them.

4.3.3 Circular Design and Simulation Results.

This method of polarization was used in order to feed a horn antenna in Figure 17. The slot used for coupling the power into the extraction waveguide resonates at 85.5 GHz. The slot arm has a width $W_a = 0.195$ mm, a short length $L_{s,a} = 0.32$ mm and a long length $L_{l,a} = 1.67$ mm. The slot is centered at 0.65 mm from the broad-wall long edge. The slot radiates into a circular waveguide with radius 2.5 mm. The radius was determined in order to only propagate a TE_{11} mode. The circular waveguide was used to feed a horn with aperture diameter, $D_a = 30$ mm and length $L_h = 45$ mm. The examination of the fields propagating inside the circular waveguide at different

instances of time showed that a degenerate TE_{11} field is propagating as shown in 18 and its scattering parameters are shown in Figure 19.

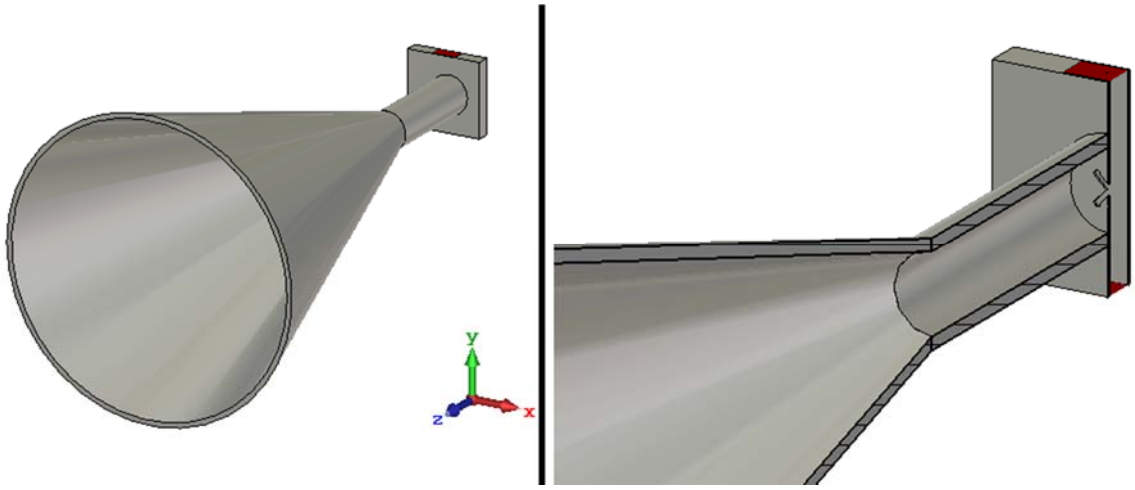

Figure 17. Horn antenna circular polarization configuration.

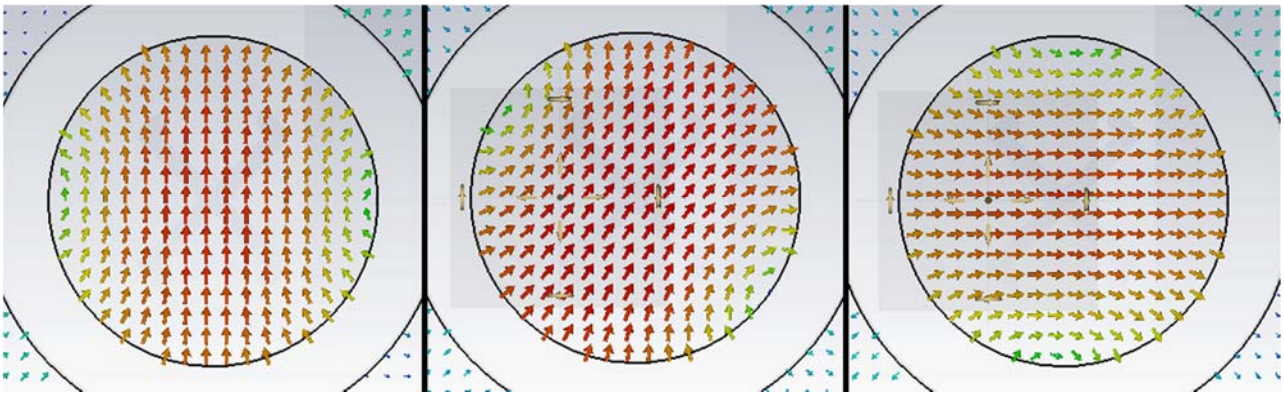

Figure 18. The E-field inside the circular waveguide at different instances of time.

Since the slot is only good for radiating power at the band of frequencies between 82- 89 GHz (50% or more of the power is radiated), the gain of the antenna is affected. The antenna radiated the most power between 83 and 88 GHz resulting in a 20 dB gain or more. Outside these frequency bands the gain dropped significantly. It was also noticed that due to the mismatch between the extraction waveguide and the feeding waveguide, the circular polarization was affected. The reflection of the radiated wave into the extraction waveguide causes the phase between the two components of the magnetic field to change and hence affecting the circular polarization and

resulting in the drop of the isolation between RH and LH CP as seen in Figure 20. This can be solved by working on a better match between the two waveguides.

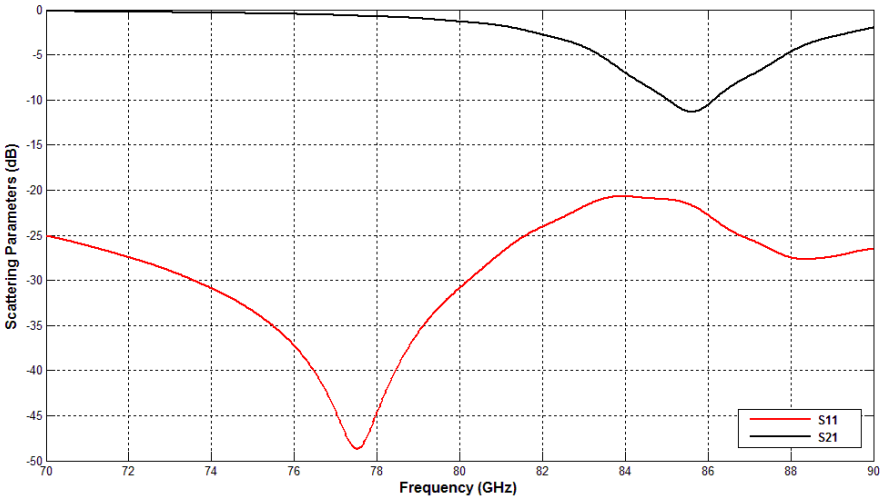

Figure 19. Horn scattering parameters.

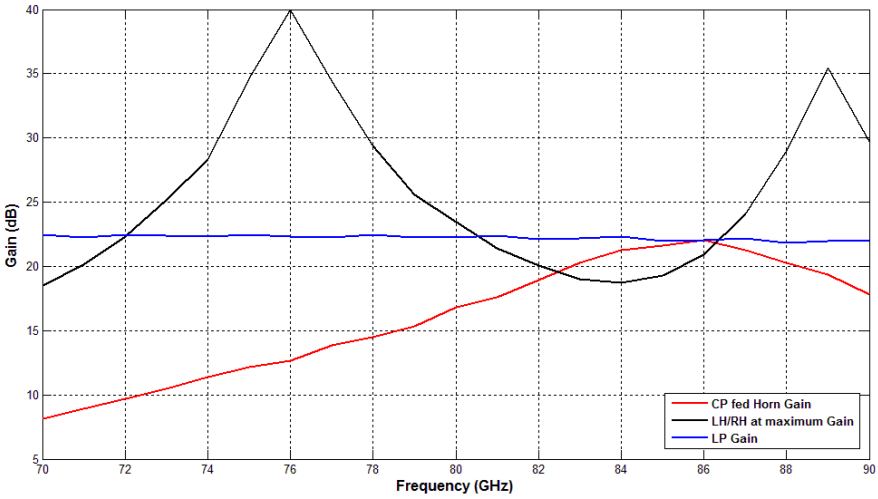

Figure 20. Horn antenna gain and the isolation between LHCP and RHCP.

Nonetheless, the radiation pattern showed that for most of the frequencies, the isolation between LHCP and RHCP was more than 20dB. As seen in Figure 21, the horn antenna has a half power beam width HPBW of 9º - 12º over the frequencies of operation. The side lobe level (SLL) is of -20 dB to -25 dB over the entire frequency range. The plot of the axial ratio over the HPBW showed that the for most of the HPBW, the axial ratio is less than 3 dB, which means that the main beam is circularly polarized for almost the entire HPBW as shown in Figure 22.

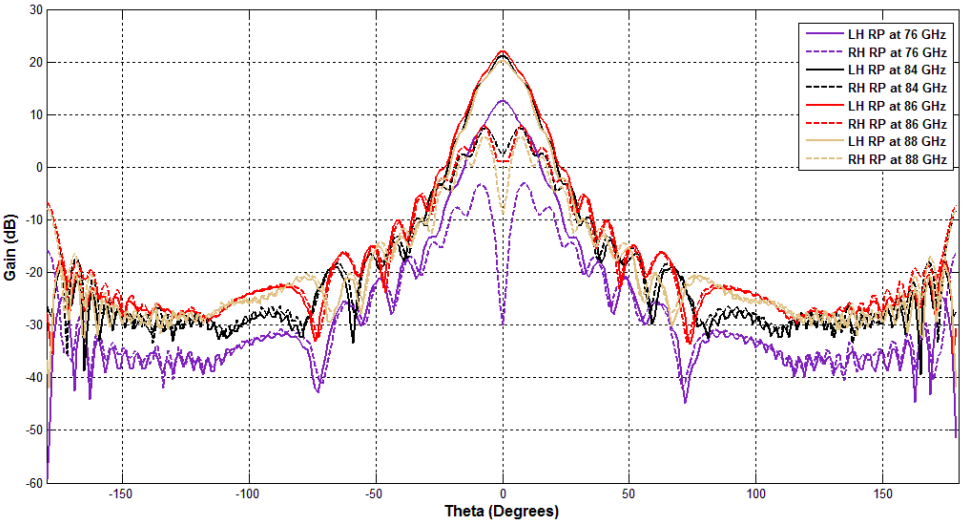

Figure 21. Radiation patterns of LH and RH CP at different frequencies.

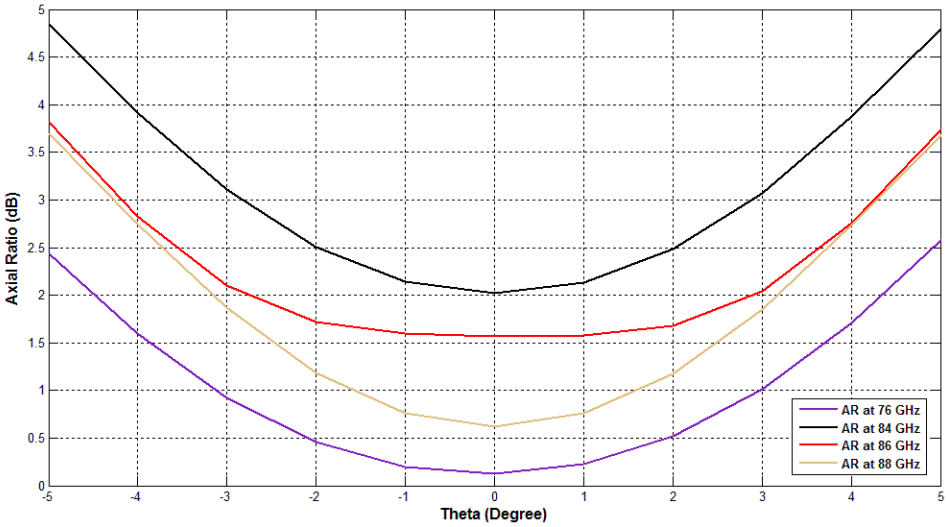

Figure 22. Axial Ratio at the HPBW in Φ=0º.

5.0 CONCLUSIONS

This report covers the research work performed on the WTLE (W/V Band Terrestrial Link Experiment) experimental link to study the propagation effects of signals at 72 and 84 GHz. The report covers the results from the data analyzed from the short link (0.56 km) to examine the validity and the accuracy of the ITU-R and Silva models for rain attenuation for the Albuquerque, New Mexico region. A preliminary antenna array design that is being developed at the W/V band that can be used in future communication links was presented and discussed in detail. Furthermore, some results from the design of a circular horn antenna for high gain performance at W/V band frequencies was include.

From the study of the models it becomes apparent that there exist several different factors that can determine the predicted attenuation for a terrestrial link. Further research will be completed to determine the degree of signal attenuation due to rain, atmospheric gases and cloud or fog attenuation. The establishment of the short link will allow us to understand the effects of weather variation over the longer WTLE experimental link.

REFERENCES

1. Recommendation ITU-R P.838-3 (2005, March), Specific attenuation model for rain for use in prediction methods. Retrieved from http://www.itu.int/rec/R-REC-P.838-3-200503-I/en.

2. Recommendation ITU-R P.676-10 (2013, September), Attenuation by atmospheric gases. Retrieved from http://www.itu.int/rec/R-REC-P.676-10-201309-I/en.

3. Recommendation ITU-R P.840-6 (2013, September), Attenuation due to clouds and fog. Retrieved from http://www.itu.int/rec/R-REC-P.840-6-201309-I/en.

4. L.A.R. da Silva Mello, M.S. Pontes, R.M. de Souza, and N.A. Perez Garcia (2007), "Prediction of rain attenuation in terrestrial links using rainfall rate distribution," Retrieved from http://ieeexplore.ieee.org/stamp/stamp.jsp?arnumber=4405611.

5. Mesowest, <http://mesowest.utah.edu/cgi bin/droman/mesomap.cgi?state=NM&rawsflag=3>, October 2014.

6. ITU-R, <http://www.itu.int/rec/R-REC-P/en>, October 2014, no author.

7. Recommendation ITU-R P.836-5 (2013, September), Water vapour: surface density and total columnar content. Retrieved from http://www.itu.int/rec/R-REC-P.836-5-201309-I/en.

8. Olsen, R., Rogers, D., and Hodge, D., "The aRb relation in the calculation of rain attenuation," pp. 318-329, 26(2), IEEE Transactions on Antennas and Propagation, April 1978, Retrieved from http://ieeexplore.ieee.org/stamp/stamp.jsp?arnumber=1141845.

9. Nessel, J.A., Acosta, R.J., Miranda, F.A., "Preliminary Experiments for the Assessment of V/W-band Links for Space-Earth Communications," 2013 IEEEAP-S/USNC-URSI Symposium, Propagation in Random or Complex Media, Orlando, FL. http://dx.doi.org/10.1109/APS.2013.6711467

10. A. Simmons, "Circularly polarized slot radiators," in *IRE Transactions on Antennas and Propagation*, vol. 5, no. 1, pp. 31-36, January 1957.

11. J. Hirokawa, M. Ando, N. Goto, N. Takahashi, T. Ojima and M. Uematsu, "A single-layer slotted leaky waveguide array antenna for mobile reception of direct broadcast from satellite," in IEEE Transactions on Vehicular Technology, vol. 44, no. 4, pp. 749-755, Nov 1995.

12. Kyeong-Sik Min; Ji-Won Ko; Arai, H.; Dong-Il Kim, "Circularly polarized array antennas with electromagnetically coupled cross slot radiator," vol. 3, pp. 1147-1150, *Microwave Conference, APMC 2001, 2001 Asia-Pacific*, Taipei, Taiwan.

13. Chatterjee, Sayan; Majumder, Arijit, "Design of circularly polarized waveguide crossed slotted array antenna at Ka band," *Microwave and Photonics (ICMAP), 2015 International Conference*, Dhanbad, Jharkhand, India.

LIST OF ACRONYMS

CDF	Cumulative Distribution Function
COSMIAC	Space Electronics Center at the University of New Mexico
dB	Decibel
dBm	Decibel with 1 mW reference
GHz	Giga-Hertz
HPBW	Half Power Beamwidth
ITU-R	International Telecommunication Union Radiocommunication Sector
km	kilo-meter
LHCP	Left-Hand Circular Polarization
mm	milli-meter
mW	Milli-Watt
RHCP	Right-Hand Circular Polarization
SLL	Side Love Level
WTLE	W/V Band Terrestrial Link Experiment

DISTRIBUTION LIST

DTIC/OCP
8725 John J. Kingman Rd, Suite 0944
Ft Belvoir, VA 22060-6218 1 cy

AFRL/RVIL
Kirtland AFB, NM 87117-5776 2 cys

Official Record Copy
AFRL/RVSW/David Murrell 1 cy